Cr^{IV}–Cr^{VI} complex. Unimolecular specific rates for this reaction, which is acid-catalyzed, conform to (7), where K_c is association

$$k_{obsd} = \frac{K_c[Cr^{VI}]}{1 + K_c[Cr^{VI}]}(k^0 + k'[H^+]) \quad (7)$$

constant for the $Cr^{VI}Cr^{IV}$ complex and k^0 and k' are the limiting specific rates (at high $[Cr^{VI}]$) for the acid-independent and $[H^+]$-proportional contributions. Refinement of specific rates according to (7) yields $K_c = (50 \pm 9)\ M^{-1}$, $k^0 = (4.3 \pm 0.5) \times 10^{-2}\ s^{-1}$, and $k' = (7.9 \pm 2.2)\ M^{-1}\ s^{-1}$. Agreement between these values and the analogous parameters pertaining to destruction of Cr(IV) formed by the reaction of $Mo_2O_4^{2+}$ with excess $Cr_2O_7^{2-}$ under similar conditions[9,15] shows that the same comproportionation process is in operation in the two systems.

In sum, several reductants that react preferentially as 2e⁻ reagents have been used to generate complexed Cr(IV) from $Cr_2O_7^{2-}$ in the aqueous buffer used. Of these, excess As(III) reacts in the most straightforward manner and gives the most stable solutions, which decay only by slow oxidation of the ligand. With $Mo_2O_4^{2+}$, U(IV), or Sn(II) in excess, Cr(IV) is reduced to Cr(III), in each case at a rate proportional to [reductant].[9,16] These conversions presumably require that the reagents assume their less usual roles as single electron donors—$Mo_2O_4^{2+}$ via unimolecular preactivation,[11] U(IV) via intervention of U(V), and Sn(II) (unexpectedly) through intermediacy of the highly atypical state Sn(III).[17] Work on the latter systems is continuing.[18]

Acknowledgment. We are grateful to Ms. Arla White for technical assistance.

(15) The corresponding values recorded for the $(Mo^V)_2$–Cr^{VI} system are as follows: $K_c = 40 \pm 7\ M^{-1}$, $k^0 = (5.3 \pm 0.8) \times 10^{-2}\ s^{-1}$, and $k' = 8.8 \pm 1.8$ (25 °C, $\mu = 0.50$ M).

(16) Ghosh, M. C. Unpublished experiments, Kent State University, 1990.
(17) Higginson, W. C. E.; Leigh, R. T.; Nightingale, R. *J. Chem. Soc.* **1962**, 435.
(18) **Note Added in Proof**: The paramagnetic susceptibilities of our chromium(IV) complexes do not appear to vary significantly with their degree of ligation. Using the procedure of D. F. Evans (*J. Chem. Soc.* **1959**, 2003), we find the effective magnetic moment, μ_{eff}, of our Cr(IV) preparations to be 2.60, 2.65, and 2.90 μ_B at $[Lig^-]$ values of 0.010, 0.16, and 0.46 M.

Contribution from the Department of Chemistry, Yale University, P.O. Box 6666, New Haven, Connecticut 06511-8118

Proton-Coupled Electron Transfer in High-Valent Oxomanganese Dimers: Role of the Ancillary Ligands

Rajesh Manchanda, H. Holden Thorp,*,† Gary W. Brudvig, and Robert H. Crabtree

Received July 17, 1990

The aqueous electrochemistry of selected binuclear mixed-valence oxo-bridged manganese clusters has been investigated. For $[Mn^{III}Mn^{IV}(O)_2(bpy)_4]^{3+}$ (**1**, bpy = 2,2′-bipyridyl), it was observed that there is a substantial isotope effect ($k_H/k_D = 4.3$) for its electrochemical reduction, consistent with the proton-coupled electron transfer observed previously. Studies on $[Mn^{III}Mn^{IV}(O)_2(edda)_2]^-$ (**2**, edda = ethylenediamine-*N*,*N*′-diacetate) show that the $E_{1/2}$ values are also pH-dependent in a manner consistent with a one-proton/one-electron (slope of 0.07 ± 0.016 V/pH, $R = 0.99$) mechanism, as with **1**. For $[Mn^{III}Mn^{IV}(O)_2(bispicen)_2]^{3+}$ (**3**, bispicen = *N*,*N*′-bis(2-methylpyridyl)ethane-1,2-diamine), similar measurements indicate an EC mechanism where the electron transfer and protonation are kinetically decoupled. The current response as a function of pH was measured to determine a $pK_a \sim 8.35$ for $[Mn^{III}_2(O)(OH)(bispicen)_2]^{3+}$. Comparison of the electrochemical properties of **1**–**3** suggests that the proton-coupled mechanism is facilitated by low steric demand of the ancillary ligands and high basicity of the oxo bridges.

Acid–base equilibria are of great importance in redox processes because they can have large effects both on thermodynamic potentials and on electron-transfer kinetics. It has been suggested that enzymatic reactions such as the binding of dioxygen and the oxidation of water and peroxide proceed via mechanisms that involve proton-coupled electron transfer at oxo-bridged metal clusters.[1,2] The study of these reactions in oxo-bridged clusters is relevant to elucidating the primary processes in the function of redox enzymes such as uteroferrin, hemerythrin, catalase, and photosystem II (PS II).[1,2] Proton-coupled redox reactions can also initiate structural rearrangements of oxomanganese clusters.[3] We have previously observed concerted transfer of an electron and a proton in an oxo-bridged dimer, $[Mn^{III}Mn^{IV}(O)_2(bpy)_4]^{3+}$ (**1**, bpy = 2,2′-bipyridyl),[4,5] which has been studied extensively as a model for the Mn cluster in PS II.[6]

Electrochemical investigations of proton-coupled electron transfer in **1** lead to quasi-reversible cyclic voltammograms and a marked dependence on the nature of the electrode surface.[4,5] Cyclic voltammetry of **1** at activated glassy-carbon electrodes gave a heterogeneous rate constant $k_s = 5 \times 10^{-3}$ cm/s at pH 3.78.[4] This value is consistent with those obtained for proton-coupled electron transfer at terminal hydroxo complexes of ruthenium.[7] The $E_{1/2}$ for voltammograms of **1** is pH-dependent ($E_{1/2}$ = (0.99–0.059 pH) V vs SSCE) in a manner consistent with the assignment of this couple to eq 1.[4] The dependence of the

$$[Mn^{III}Mn^{IV}(O)_2(bpy)_4]^{3+} + e^- + H^+ \rightarrow [Mn^{III}_2(O)(OH)(bpy)_4]^{3+} \quad (1)$$

heterogeneous kinetics of this reaction on the nature of the electrode surface is remarkable,[4,5] as it is for other proton-coupled reactions.[7] Voltammetric results for activated glassy carbon, tin-doped indium oxide, and edge-oriented pyrolytic graphite are consistent with a model where specific sites on the electrode surface mediate proton transfer to the metal complex.[5] Thus, a special interaction between the metal complex and the surface site is

† Present address: Department of Chemistry, North Carolina State University, Raleigh, NC 27695-8204.

(1) (a) Brudvig, G. W.; Crabtree, R. H. *Prog. Inorg. Chem.* **1989**, *37*, 99. (b) Vincent, J. B.; Christou, G. *Adv. Inorg. Chem.* **1989**, *33*, 197. (c) Brudvig, G. W.; Beck, W. F.; dePaula, J. C. *Annu. Rev. Biophys. Chem.* **1989**, *18*, 25. (d) Chan, M. K.; Armstrong, W. H. *J. Am. Chem. Soc.* **1990**, *112*, 4985.
(2) Lippard, S. J. *Angew. Chem., Int. Ed. Engl.* **1988**, *27*, 344.
(3) Sarneski, J. E.; Thorp, H. H.; Brudvig, G. W.; Crabtree, R. H.; Schulte, G. K. *J. Am. Chem. Soc.* **1990**, *112*, 7255.
(4) Thorp, H. H.; Sarneski, J. E.; Brudvig, G. W.; Crabtree, R. H. *J. Am. Chem. Soc.* **1989**, *111*, 9249.
(5) Thorp, H. H.; Bowden, E. F.; Brudvig, G. W. *J. Electroanal. Chem. Interfacial Electrochem.* **1990**, *290*, 293.
(6) (a) Cooper, S. R.; Calvin, M. *J. Am. Chem. Soc.* **1977**, *99*, 6623. (b) Cooper, S. R.; Dismukes, G. C.; Klein, M. P.; Calvin, M. *J. Am. Chem. Soc.* **1978**, *100*, 5248.
(7) Cabaniss, G. E.; Diamantis, A. A.; Murphy, W. R., Jr.; Linton, R. W.; Meyer, T. J. *J. Am. Chem. Soc.* **1985**, *107*, 1845.

0020-1669/91/1330-0494$02.50/0

required for coupling of the protonation event to the electron transfer. This situation is likely to be analogous to the active site of redox enzymes where a basic residue may be available for deprotonation of the hydroxo-bridged catalyst concomitant with oxidation.[1,2]

Recent work by Rush and Maskos[8] on the dismutation of peroxide by Mn complexes has shown that stable solutions of $[Mn^{III}Mn^{IV}(O)_2(edda)_2]^-$ (**2**, edda = ethylenediamine-*N*,*N*′-diacetate) can be prepared in the pH 6–7 range. The EPR spectra of these solutions show 16-line signals centered at $g = 2$ that are diagnostic of the III,IV oxidation state. Hodgson et al.[9] have studied the aqueous electrochemistry of $[Mn^{III}Mn^{IV}(O)_2(bispicen)_2]^{3+}$ (**3**, bispicen = *N*,*N*′-bis(2-methylpyridyl)ethane-1,2-diamine). At high pH, the cyclic voltammogram of **3** exhibits two reversible waves at 0.15 and 0.75 V (SCE) corresponding to the III,III/III,IV and III,IV/IV,IV couples, respectively. At low pH, the III,III/III,IV couple is replaced by an irreversible two-electron wave near the same potential.

We present here a comparative study of the aqueous electrochemistry of **1**–**3**, which demonstrates that the ancillary ligands play a significant role in regulating proton-coupled electron transfer in oxo-bridged systems. We have measured the cyclic voltammogram of **1** in D_2O and find that there is a significant kinetic isotope effect, consistent with the proton-coupled electron transfer of eq 1. The voltammetry of **2** confirms that reduction of this complex is also proton-coupled, in a manner analogous to **1**. The reduction of **3** is also accompanied by protonation; however, in this system the protonation is not coupled to the electron transfer but occurs as a following chemical reaction in an EC-type mechanism.[10]

Experimental Section

Electrochemistry. Cyclic voltammograms were recorded in Milli-Q water by using a PAR 273 potentiostat. Glassy-carbon working electrodes were activated in 0.1 M H_2SO_4 by cycling the potential between +1.8 V (30 s) and −0.2 V (15 s) after polishing with alumina.[7] The auxiliary electrode was a Pt wire with a SSCE reference electrode. Complex concentration was 1–2 mM. The solutions were buffered with either phosphate, edda (Aldrich), or bispicen (prepared by a literature[11] method). The pH was adjusted after addition of the metal complex by adding 0.1 M NaOH or 0.1 M $HClO_4$. NaD_2PO_4 was prepared by lyophilizing NaH_2PO_4 three times in D_2O, yielding an isotopic purity of at least 99%.

Complexes. $[Mn_2(O)_2(bpy)_4]^{3+}$ [6a] and $[Mn_2(O)_2(bispicen)_2]^{3+}$ [12] were prepared by published procedures. Solutions of $[Mn_2(O)_2(edda)_2]^-$ were prepared in situ by addition of **1** to a 0.05 M solution of edda according to Rush and Maskos.[8]

Results and Discussion

$[Mn^{III}Mn^{IV}(O)_2(bpy)_4]^{3+}$. Kinetic Isotope Effect. The cyclic voltammogram of **1** at pH 4.4 (0.1 M NaH_2PO_4) is shown in Figure 1A. The heterogeneous charge-transfer rate determined from ΔE_p is $k_s = 3.1 \times 10^{-3}$ cm/s according to the method of Nicholson;[13] we previously reported that the peak currents are a linear function of the square root of the scan rate.[4] The assignment of this couple to eq 1 would suggest that a large kinetic isotope effect should be observed. Figure 1B shows the cyclic voltammogram of **1** in D_2O with 0.1 M NaD_2PO_4. The large isotope effect is evident in the broadening of both the oxidative and reductive components of the wave. The heterogeneous charge-transfer rate for D_2O is $k_s = 1.5 \times 10^{-3}$ cm/s by the same method.[13] The heterogenous rate constants were converted to homogeneous rate constants (units of M^{-1} s^{-1}) by application of Marcus theory.[14a] The ratio of the homogeneous rate constants

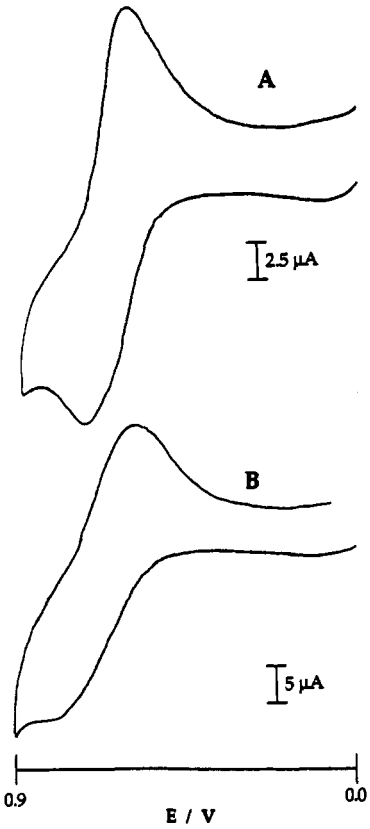

Figure 1. Cyclic voltammograms of $[Mn_2(O)_2(bpy)_4]^{3+}$: (A) 0.1 M NaH_2PO_4 in H_2O; (B) 0.1 M NaD_2PO_4 in D_2O. Scan rate: 100 mV/s.

was used to determine a k_H/k_D of 4.3. This value is in agreement with isotope effects for other H atom transfer reactions.[14b] A substantial kinetic isotope effect has also been observed for $[Ru(NH_3)_5(OH)]^{2+}$ associated with eq 2.[7]

$$[Ru^{IV}(NH_3)_5(O)]^{2+} + H^+ + e^- \rightarrow [Ru^{III}(NH_3)_5(OH)]^{2+} \quad (2)$$

The large k_H/k_D emphasizes the intimate connection between proton transfer and electron transfer in **1**. This observation is consistent with the slow electrode kinetics resulting from the coupling of the protonation to the redox reaction.[4,5] From our experiments on other electrode surfaces, it appears that some degree of deprotonated oxide functionality is required for efficient mediation of proton-coupled electron transfer. In our model, proton transfer to the metal complex occurs from a site on the electrode surface; blocking this site by protonation of the surface or strong adsorption of the metal complex has been shown to prohibit electron transfer on indium oxide.[5] This model is supported by the observation of a substantial kinetic isotope effect for eq 1.

$[Mn^{III}Mn^{IV}(O)_2(edda)_2]^-$. The one-electron reduction of **2** was previously studied by pulse radiolysis.[8] The results were consistent with the formation of a III,III complex but did not indicate whether a protonation event occurred. The III,III product was observed to disproportionate to $Mn^{II} + Mn^{IV}$ at a rate of 0.3 s^{-1}. Thus, the electrochemical observation of the III,III/III,IV couple in this system requires scan rates sufficiently high to compete with the decomposition of the III,III complex. In proton-coupled reactions, an additional complication arises from the slow electrode kinetics, which will greatly broaden voltammograms taken at higher scan rates.[13] The cyclic voltammogram of **2** taken at 200 mV/s is shown in Figure 2. The slow electrode kinetics result in broad waves with a large ΔE_p, although this splitting is near that for **1** at this scan rate.[15] Despite the breadth of these waves, it was possible to obtain $E_{1/2}$ values in the pH range 5.8–7.4 that were reproducible to ±0.01 V.

(8) Rush, A. J.; Maskos, Z. *Inorg. Chem.* **1990**, *29*, 897.
(9) Goodson, P. A.; Glerup, J.; Hodgson, D. J.; Michelsen, K.; Pedersen, E. *Inorg. Chem.* **1990**, *29*, 503.
(10) Nicholson, R. S.; Shain, I. *Anal. Chem.* **1964**, *36*, 706.
(11) Michelsen, K. *Acta. Chem. Scand.* **1977**, *A31* (No. 6), 430.
(12) Collins, M. A.; Hodgson, D. J.; Michelsen, K.; Towle, D. K. *J. Chem. Soc., Chem. Commun.* **1987**, 1659.
(13) Nicholson, R. S. *Anal. Chem.* **1965**, *37*, 1351.
(14) (a) Southhampton Electrochemistry Group. *Instrumental Methods in Electrochemistry*; Ellis Horwood: Chichester, England, 1985. (b) Turro, N. J. *Modern Molecular Photochemistry*; Benjamin/Cummings: Menlo Park, CA, 1978.
(15) Thorp, H. H.; Brudvig, G. W. Unpublished results.

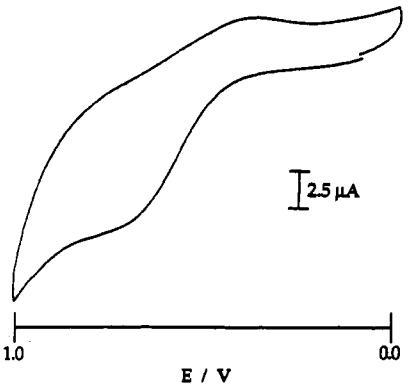

Figure 2. Cyclic voltammogram of $[Mn_2(O)_2(edda)_2]^-$ in 0.05 M edda at pH 5.94. Scan rate: 200 mV/s.

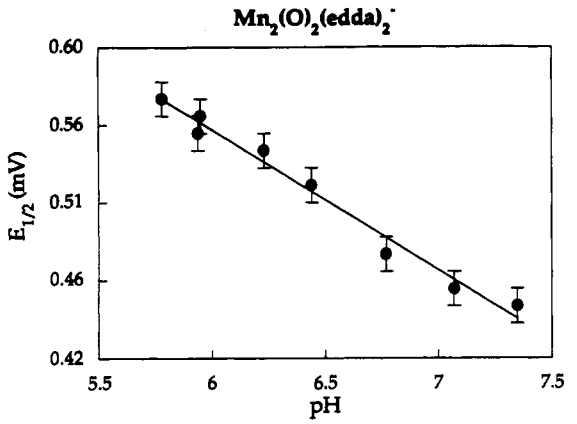

Figure 3. Pourbaix diagram for $[Mn_2(O)_2(edda)_2]^-$.

It has been reported[8] that solutions of **2** are stable in the pH range 6–7, and we were able to make reliable measurements in approximately the same range. The pH dependence of the $E_{1/2}$ for the voltammogram of **2** is given in the Pourbaix diagram shown in Figure 3. Pourbaix diagrams are useful for determining the number of protons involved in a given redox reaction, according to the Nernst equation. The pH dependence shown in Figure 3 is linear (R = 0.99) with a slope of −0.07 ± 0.016 V/pH unit, which is equal within experimental error to −0.059 V required for a one-electron/one-proton redox couple. We therefore assign this process to the $Mn_2(O)_2^{3+}/Mn_2(O)(OH)^{3+}$ couple shown in eq 3. Thus, proton-coupled electron transfer is not specific to **1** and can occur in other oxo-bridged dimers.

$$[Mn^{III}Mn^{IV}(O)_2(edda)_2]^- + H^+ + e^- \rightarrow [Mn^{III}_2(O)(OH)(edda)_2]^- \quad (3)$$

$[Mn^{III}Mn^{IV}(O)_2(bispicen)_2]^{3+}$. The aqueous electrochemistry of **3** reported by Hodgson et al.,[9] shows at 0.15 V a reversible III,III/III,IV couple at pH 7.4 in 0.1 M $NaClO_4$. At pH 2.4, this couple is replaced by an irreversible two-electron wave at about the same potential. We attempted to investigate this pH region in more detail in order to understand the role of protonation in this transition. We have found that reliable pH measurements require the presence of an electrolyte that can act as a buffer in the relevant pH regime. The complex is unstable in coordinating buffers such as phosphate and acetate, but in the presence of excess bispicen ligand, the solutions are stable and buffered. Similar observations were reported by Cooper and Calvin[6] for **1**, where a bipyridyl buffer was used to stabilize the III,IV form in aqueous solution.

We have investigated the pH dependence of the voltammetry of **3** in 0.1 M bispicen buffer in the pH range 7.6–9. The presence of the bispicen buffer is required to obtain a stable pH, which accounts for the discrepancy between our pH values and those measured in 0.1 M $NaClO_4$.[9] We observe the quasi-reversible III,III/III,IV couple at pH 8.9 in 0.1 M bispicen (Figure 4A),

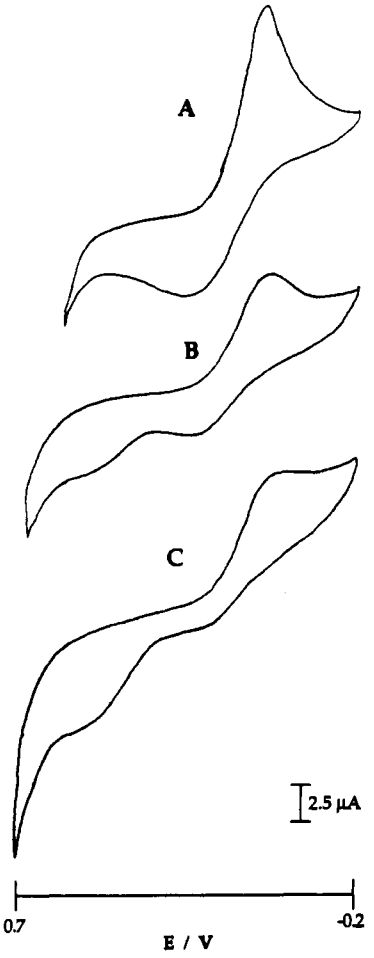

Figure 4. Cyclic voltammograms of $[Mn_2(O)_2(bispicen)_2]^{3+}$ in 0.1 M bispicen: (A) pH 8.9; (B) pH 8.1; (C) pH 7.6. Scan rate: 100 mV/s.

with the III,IV/IV,IV wave obscured by the background resulting from the higher pH.

As the pH is lowered, the III,III/III,IV couple gradually becomes irreversible while a new peak appears at ~0.5 V (Figure 4B). By pH 7.6, the oxidative component of the III,III/III,IV couple has disappeared, and the new peak is at a maximum (Figure 4C). The current response at pH 7.6 remains consistent with a one-electron reduction. We have reproduced these observations in 0.1 M $NaClO_4$ and obtain results consistent with those of Hodgson,[9] although the pH of ClO_4^- solutions is not as stable. The behavior shown in Figure 4 was also observed in 0.1 M $NaClO_4$, but the measured pH values were ~1.5 units lower than those in Figure 4. In 0.1 M $NaClO_4$, the III,IV/IV,IV couple at 0.75 V was visible above the solvent background in the pH range studied, and the peak morphology of this oxidation wave remained constant. At low pH, an abrupt transition occurs between the behavior of Figure 4C and the irreversible two-electron wave observed by Hodgson et al.[9] The voltammetric behavior in Figure 4 is ascribed to the mechanism shown in eq 4–7. The starting

$$[Mn^{III}Mn^{IV}(O)_2(bispicen)_2]^{3+} + e^- \rightarrow [Mn^{III}_2(O)_2(bispicen)_2]^{2+} \quad (4)$$

$$[Mn^{III}_2(O)_2(bispicen)_2]^{2+} + H^+ \rightarrow [Mn^{III}_2(O)(OH)(bispicen)_2]^{3+} \quad (5)$$

$$[Mn^{III}_2(O)(OH)(bispicen)_2]^{3+} \rightarrow [Mn^{III}Mn^{IV}(O)(OH)(bispicen)_2]^{4+} + e^- \quad (6)$$

$$[Mn^{III}Mn^{IV}(O)(OH)(bispicen)_2]^{4+} \rightarrow [Mn^{III}Mn^{IV}(O)_2(bispicen)_2]^{3+} + H^+ \quad (7)$$

potential was 0.5 V, and after scanning negatively, the III,IV complex is reduced by one electron at $E_p \sim 0.05$ V (eq 4). At

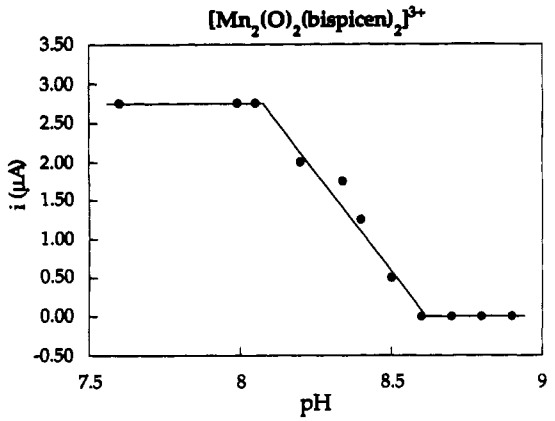

Figure 5. pH dependence of the current of the peak at 0.5 V in microamps for $[Mn_2(O)_2(bispicen)_2]^{3+}$.

pH ≥ 8.6, the wave is quasi-reversible, with the reoxidation visible on the return scan (Figure 4A). As the pH is lowered, the current for the reoxidation is decreased because of a follow-up reaction involving protonation of the III,III product, as in eq 5 (Figure 4B). This decrease is accompanied by the appearance of a new oxidation wave at ~0.5 V, which we assign to oxidation of the protonated III,III species (eq 6). This species then deprotonates (eq 7) in a follow-up reaction and is available for oxidation to the IV,IV level at 0.75 V, as has been observed.

Our mechanism is supported by a number of observations. First, if the new wave at 0.5 V arises from a protonated species, as shown in eq 6, the current for this wave should follow a characteristic pH titration dependence. This is indeed the case, as shown in Figure 5. From these data, we estimate a pK_a of 8.35 for the $[Mn^{III}_2(O)(OH)(bispicen)_2]^{3+}$ species. Second, in 0.1 M $NaClO_4$ medium, the current response for the III,IV/IV,IV couple at 0.75 V is invariant with pH. Thus, the III,IV complex is always fully regenerated prior to reaching the oxidation potential for the III,IV complex, as would occur in our mechanism. Finally, the broadening of the III,III/III,IV reduction peak at 0.05 V is consistent with electrode adsorption of the III,III product, and we have observed that $[Mn^{III}_2(O)(OH)(bpy)_4]^{3+}$ is adsorbed under certain conditions.[5]

The proton-coupled reduction in **1** and **2** contrasts with the EC mechanism for **3**, which involves one-electron reduction followed by protonation in a separate step.[10] This may be a result of the greater steric demand of the bispicen ligand relative to bpy and edda. Thus, in the bispicen complex, the oxo groups may not be free to interact with the electrode surface, which we have shown is required for proton-coupled electrochemistry to be observed.[5] Generation of space-filling models from the coordinates in the Cambridge Data Base show that in **3**,[12] the $-CH_2-$ groups bridging the amines and the pyridine rings are close to the oxo group. Inspection of these models suggests that these methylene protons may prohibit access of the oxo groups to the electrode surface. In **1**,[16] however, the planar bpy ligand is forced away from the oxo groups, and free interaction with the electrode surface might be possible.

An additional explanation for the failure of **3** to exhibit proton-coupled electrochemistry may be evident in the measured pK_a.[17,18] We have previously estimated the pK_a of $[Mn^{III}_2(O)(OH)(bpy)_4]^{3+}$ to be 11.0.[4] The pK_a of 8.3 reported here for $[Mn^{III}_2(O)(OH)(bispicen)_2]^{3+}$ shows that the oxo bridges of **3** are significantly less basic than those in **1**. Favorable orientation of the complex on the electrode surface may be encouraged by a strongly basic oxo bridge, which will be a good H-bond acceptor. The oxo bridges in **3** may not sufficiently encourage favorable orientation of the complex on the electrode surface to permit efficient electrocatalysis of the proton-coupled reaction.[5,7]

Conclusions

We have presented two extremes in the interplay between redox chemistry and protonation in oxo-bridged manganese clusters, as dictated by the nature of the ancillary ligands. In **1** and **2**, the protonation event is coupled to the redox reaction, resulting in pH-dependent $E_{1/2}$ values and reactions that are quite sensitive to the ability of the electrode surface to mediate the proton transfer. This intimate coupling of redox and acid–base chemistry is emphasized by the large kinetic isotope effect for **1**. In the other extreme observed for **3**, the protonation and electron-transfer events are kinetically decoupled, giving the voltammetric behavior shown in Figure 4. This may result from blockage of the oxo groups by the sterically demanding bispicen ligand or the lower basicity of the oxo bridges in **3**.

We have pointed out that proton-coupled electron transfer offers thermodynamic and kinetic control to enzymes containing oxo-bridged metal clusters at their active sites.[1c,4] The Pourbaix diagrams demonstrate that, through control of the effective pH, the thermodynamics of proton-coupled electron transfer can be controlled. These new results suggest that kinetic control can be obtained by providing a facile mechanism for the catalysis of proton-coupled reactions in redox enzymes. In these relevant enzymes, if a basic residue is proximal to a protonated oxo bridge, then proton-coupled redox chemistry may be effected, as in **1** and **2**. On the other hand, if the relevant site is blocked, outer-sphere electron transfer may precede a separate proton-transfer step, as observed for **3**.

Acknowledgment. We thank Professor Joseph E. Sarneski (Fairfield University) for preparing **1** and **3**. We also thank Professor Edmond F. Bowden for helpful discussions. This research was supported by the National Institutes of Health through Grants GM-32715 and GM-40974 and the Cooperative State Research Service, U.S. Department of Agriculture, under Agreement No. 90-37130-5575.

(16) Plaskin, P. M.; Stoufer, R. C.; Mathew, M.; Palenik, G. J. *J. Am. Chem. Soc.* **1972**, *94*, 2121.
(17) We are grateful to a reviewer for this suggestion.
(18) Binstead, R. A.; Meyer, T. J. *J. Am. Chem. Soc.* **1987**, *109*, 3287.